Mesomorphic behaviour in copoly(ester-imide)s of poly(butylene-2,6-naphthalate) (PBN)

Polymer 69 (2015) 66–72

Contents lists available at ScienceDirect

Polymer

journal homepage: www.elsevier.com/locate/polymer

Mesomorphic behaviour in copoly(ester-imide)s of poly(butylene-2,6-naphthalate) (PBN)

Stephen M. Jones [a], Stephen J. Meehan [a], Stephen W. Sankey [b], William A. MacDonald [b], Howard M. Colquhoun [a, *]

[a] Department of Chemistry, University of Reading, Whiteknights, Reading, RG6 6AD, UK
[b] DuPont Teijin Films UK Ltd., Wilton Centre, Redcar, North Yorkshire, TS10 4RF, UK

ARTICLE INFO

Article history:
Received 9 March 2015
Received in revised form
11 May 2015
Accepted 13 May 2015
Available online 21 May 2015

Keywords:
Liquid crystal
Poly(butylene-2,6-naphthalate)
Glass transition temperature

ABSTRACT

Copolycondensation of *N*,*N*′-bis(4-hydroxybutyl)-biphenyl-3,4,3′,4′-tetracarboxylic diimide at 20 and 25 mol% with bis(4-hydroxybutyl)-2,6-naphthalate produces PBN-based copoly(ester-imide)s that not only crystallise but also form a (smectic) mesophase upon cooling from the melt. Incorporation of 25 mol % imide in PBN causes the glass transition temperature (measured by DSC) to rise from 51 to 74 °C, a significant increase relative to PBN. Furthermore, increased storage- (G′), loss- (G″) and elastic (E) moduli are observed for both copoly(ester-imide)s when compared to PBN itself. Structural analysis of the 20 mol% copolymer by X-ray powder and fibre diffraction, interfaced to computational modelling, suggests a crystal structure related to that of α-PBN, in space group $P-1$, with cell dimensions $a = 4.74$, $b = 6.38$, $c = 14.45$ Å, $\alpha = 106.1$, $\beta = 122.1$, $\gamma = 97.3°$, $\rho = 1.37$ g cm^{-3}.

1. Introduction

Semi-crystalline, semi-aromatic polyesters such as poly(ethylene terephthalate) (PET), poly(ethylene 2,6-naphthalate) (PEN) and poly(1,4-butylene terephthalate) (PBT) have found widespread use as engineering polymers in film and fibre form, and (for PBT) in moulding applications, due to their high mechanical strength, chemical resistance and dimensional stability [1]. Most recently, poly(1,4-butylene 2,6-naphthalate) (PBN) has been introduced as a fast-crystallising polyester with enhanced thermomechanical characteristics relative to PBT [2]. However, the thermal performance of semi-aromatic polyesters remains relatively low in comparison to high-temperature engineering thermoplastics such as polyetheretherketone (PEEK), with the glass transition temperatures, T_gs, of semi-aromatic, semi-crystalline polyesters being generally considered the limiting factor in terms of future product innovation in this field [3–5].

An apparently straightforward approach to enhancing the thermomechanical properties of a polymer involves copolymerisation with a more rigid comonomer, in order to increase the T_g. This technique has been employed previously in semi-aromatic polyester chemistry, most commonly utilising rigid biphenylene [6,7] and diimide moieties [8,9]. Modest increases in T_g were indeed obtained, but almost invariably with little or no retention of crystallinity in the resulting copolymers. Such copolymers would be inadequate for film applications requiring the mechanical strength achieved from biaxial orientation. It would therefore be preferable to use a rigid comonomer that is also isomorphic with the homopolymer repeat unit, enabling the copolymer to crystallise from the melt at any comonomer composition ratio. It has, for example, been observed that the copolymers of PBN with PEN [10] and PBN with PBT [11] co-crystallise across a wide composition range.

In contrast to PET [12], PBT [13], and PEN [14], there have been relatively few investigations of the melt-crystallisation processes and resulting morphology of PBN. However, it has been reported that PBN is capable of adopting two different crystal structures on cooling from the melt, referred to as the α-form and the β-form [15]. The α-form is obtained at moderate cooling rates (20–50 °C min^{-1}) from temperatures lower than 205 °C whereas the β-form is exclusively present after very slow cooling (0.1 °C min^{-1}) from above 280 °C. Both forms may co-exist after melt-crystallisation from close to the crystalline melting temperature, T_m, of PBN (238 °C) [15].

In addition, a mesophase has been reported for PBN upon very rapid quenching from the melt to 0 °C. The liquid crystalline phase has been characterised as smectic A, with a layer-periodicity of ca.

* Corresponding author. Tel.: +44 (0) 118 378 6717.
E-mail address: h.m.colquhoun@reading.ac.uk (H.M. Colquhoun).

http://dx.doi.org/10.1016/j.polymer.2015.05.025

14 Å, corresponding closely to the length of the molecular repeat unit [16]. This polyester thus displays the characteristics of both a semi-crystalline and a mesomorphic material, depending on the conditions of melt-processing. In the present work we report a novel series of PBN-based cocrystalline copoly(ester-imide)s that display both significantly higher T_gs than PBN itself, and a more accessible mesophase.

2. Experimental

2.1. Materials and synthesis

3,4,3′,4′-Biphenyltetracarboxylic dianhydride was purchased from TCI UK, and 4-aminobutanol was obtained from Alfa Aesar UK. Sb_2O_3 was purchased from SICA, France. Dimethyl 2,6-naphthalate was provided by DuPont Teijin Films UK.

Comonomer **1** (Scheme 1) was obtained by adding 4-amino-1-butanol (9.92 g, 0.11 mol) dropwise to a solution of biphenyl-3,4,3′,4′-tetracarboxylic dianhydride (15.82 g, 0.05 mol) in DMF (250 mL). The reaction mixture was heated to reflux for 16 h. After cooling to room temperature, the solution was poured into deionised water to form a precipitate, which was filtered off and dried under vacuum at 80 °C for 24 h to afford the product (20.54 g, 89%).

Bis(4-hydroxybutyl)-2,6-naphthalate was synthesised by heating a solution of dimethyl 2,6-naphthalate (242 g, 0.99 mol), 1,4-butanediol (267 g, 2.96 mol) and titanium isopropoxide (0.04 g, 0.14 mmol) to 230 °C over a 2 h period before being held at this temperature for a further 2 h. The reaction solution was then cooled to room temperature and poured into deionised water to form a precipitate which was filtered off and dried under vacuum at 80 °C for 24 h to afford the product (321 g, 90%).

The PBN-based copoly(ester-imide)s **2** were synthesised (Scheme 1) by melt-copolycondensation of bis(4-hydroxybutyl)-2,6-naphthalate with **1**. The composition of copolymer **2** was varied by changing the molar feed ratios of bis(4-hydroxybutyl)-2,6-naphthalate and **1**. A typical melt copolycondensation procedure (20 mol% copolymer) was carried out as follows. A polymerisation tube loaded with bis(4-hydroxybutyl)-2,6-naphthalate (33.33 g, 0.093 mol), comonomer **1** (10.09 g, 0.023 mol) and Sb_2O_3 (0.10 g, 0.34 mmol) was fitted with a tube-head having gas, vacuum and stirrer inlets and was placed inside a vertical tube furnace with a glass stirrer rod attached to a mechanical stirrer. The reaction mixture was heated to 200 °C under a nitrogen atmosphere over 30 min at a stirring speed of 300 rpm. The temperature was then increased to 270 °C over 40 min, with a progressive reduction in pressure to <1 mbar, and the co-produced 1,4-butanediol collected in a cold trap between the reactor and the vacuum pump. After stirring for a further 1 h at 270 °C, the resulting copolymer was cooled, dissolved from the Schlenk tube in chloroform/trifluoroacetic acid (TFA), 2:1 v/v, and reprecipitated in methanol. The copolymer was recovered by filtration and dried under vacuum at 120 °C for 24 h, giving copolymer **2** (30.32 g, 86%). Full characterisation details of the monomers and polymers synthesised in this work are given in the Supplementary data.

2.2. Monomer and polymer characterisation

^1H and ^{13}C NMR spectra were obtained on a Bruker Nanobay 400 spectrometer in the mixed solvent $CDCl_3$:TFA (2:1 v/v). Mass spectra were obtained on a LTQ Orbitrap XL with an Accela LC autosampler. Infrared spectra were obtained on a Perkin Elmer Spectrum 100 FT-IR spectrometer with a Universal Attenuated Total Reflectance accessory. Inherent viscosities (η_{inh}) were measured at 25 °C for 0.1 wt% polymer solutions in the mixed solvent $CHCl_3$:TFA (2:1 v/v) using a Schott-Geräte CT-52 auto-viscometer.

Gel permeation chromatography (GPC) was performed on a Viscotek GPC Max instrument using 2 × 30 cm HFPGel columns at 40 °C. Hexafluoropropan-2-ol (HFIP) was used as eluent for samples at a concentration of 4 mg mL^{-1}, with a flow rate of 0.7 mL min^{-1}. Molecular weights were referenced to polystyrene standards. Polarised optical microscopy was performed on a Leica DMRX compound microscope. Isotropic sample pellets were immersed in a liquid of refractive index 1.600 on a glass side prior to examination.

Rotational rheology analysis was performed on a Rheometric rheometer. Polymer samples (~2.5 g) were dried under vacuum at

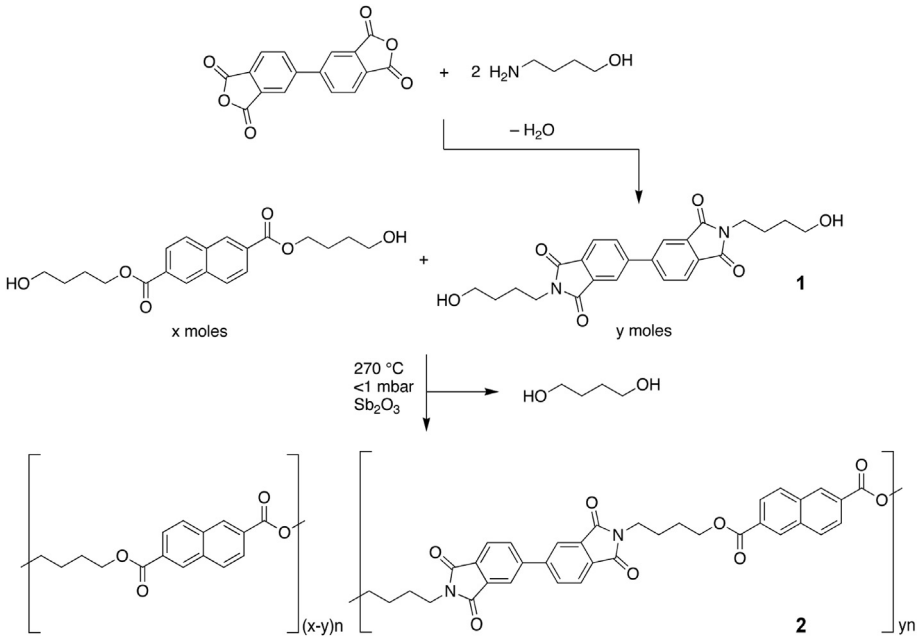

Scheme 1. Synthesis of PBN-based copoly(ester-imide)s **2** via melt-copolycondensation of bis(4-hydroxybutyl)-2,6-naphthalate with the comonomer *N*,*N*′-bis(4-hydroxybutyl)-biphenyl-3,4,3′,4′ tetracarboxylic diimide, **1**.

140 °C for 16 h prior to being placed between 2 × 25 mm diameter parallel plates and heated to the required temperature under a nitrogen atmosphere. Measurements were taken every 30 s. In temperature sweep mode, samples were heated from above the T_m to 350 °C at 4 °C min^{-1} at constant frequency (10 rad s^{-1}) and strain amplitude (5%). In frequency sweep mode, samples were subject to a change in frequency (between 0.1 and 100 rad s^{-1}) at constant temperature (300 °C) and strain amplitude (25%).

2.3. Thermomechanical analysis

Thermal transitions were analysed by DSC under a nitrogen atmosphere with a flow rate of 50 mL min^{-1}. Crystallisation exotherm peaks were obtained on cooling scans from the isotropic melt. Samples cooled at 20 °C min^{-1} were analysed using a TA Instruments DSC Q2000 instrument, whereas those requiring cooling at rates of >20 °C min^{-1} were analysed using a PerkinElmer HyperDSC 8500. Glass transition temperatures were measured as the onset temperatures at heating rates of 20 °C min^{-1} following ballistic cooling (~900 °C min^{-1}) from the isotropic melt using a PerkinElmer HyperDSC 8500.

Dynamic mechanical analysis (DMA) was performed on a TA Q800 DMA using a frequency of 10 Hz and strain of 0.1%. Fibre samples were held in place using tensile clamps before being heated from 0 to 150 °C at a rate of 4 °C min^{-1}. Elastic moduli were obtained from fibre samples on an Instron Model 4464 using a gauge length of 50 mm. Final recorded values are expressed as the mean of at least 5 measurements per fibre sample.

2.4. X-ray diffraction and computational modelling

X-ray powder diffraction patterns were obtained in transmission mode on an Oxford Diffraction Gemini Ultra diffractometer using Cu-Kα radiation (λ = 1.5418 Å), with 90° φ rotations over the 2θ range 5–50°. Intensity data were merged, corrected for absorption, and amorphous scattering removed using CrysalisPro7 software, before the powder diffraction data were circularly integrated to give one-dimensional powder patterns.

X-ray powder diffraction data for structural analysis and modelling were obtained from a finely powdered sample that had been annealed for 2 h at 180 °C, sieved through a 300 μm screen, and loaded into a 0.3 mm Lindemann capillary tube that was then spun in the X-ray beam. Capillary mode diffraction data were collected at room temperature using a Bruker D8 powder diffractometer using Cu-Kα$_1$ radiation (λ = 1.5406 Å) over the 2θ range 5–60°. The amorphous scattering component was removed from the data before these were used for direct comparison with simulated powder data from computational models.

Polymer fibres were obtained by manually drawing quenched samples at 100 °C to ca. 5× extension. X-Ray fibre patterns were obtained using a Rigaku/MSC FR-D X-ray source (Cu-Kα, λ = 1.5418 Å) and a Saturn 92 CCD detector. Data were collected for 45 s with a sample-to-plate distance of 50 mm and the X-ray beam normal to the axis of the fibre.

Model building, powder diffraction simulation, and Pawley and Rietveld refinement were undertaken using Materials Studio software (v. 7.0, Accelrys, San Diego, USA). Energy minimisation of polymer structures was carried out using the Accelrys Universal force field. X-ray fibre diagrams were simulated from the final structure using Cerius2 software (v. 3.5, Accelrys, San Diego, USA).

3. Results and discussion

Here we report on the synthesis of a novel group of PBN-based copoly(ester-imide)s and evaluate their potential as new high performance materials. This work builds on previous research which showed that copolycondensation of *N*,*N*′-bis(2-hydroxyethyl)-biphenyl-3,4,3′,4′-tetracarboxylic diimide with bis(2-hydroxyethyl)-2,6-naphthalate afforded a series of semi-crystalline PEN-based copoly(ester-imide)s [17]. Such copolymers showed both enhanced T_gs and retention of semi-crystalline behaviour, from which it was evident that the two different co-monomers are able to cocrystallise. It was thus envisaged that copolymerisation of bis(4-hydroxybutyl)-2,6-naphthalate with *N*,*N*′-bis(4-hydroxybutyl)-biphenyl-3,4,3′,4′-tetracarboxylic diimide might well produce cocrystalline, PBN-based copoly(ester-imide)s with significantly higher T_gs than the homopolymer.

Considering the overall dimensions of the two comonomers involved, the notion of co-crystallisation appears entirely feasible. Fig. 1 illustrates the potentially isomorphic nature of *N*,*N*′-bis(4-hydroxybutyl)-biphenyl-3,4,3′,4′-tetracarboxylic diimide **1** and bis(4-hydroxybutyl)-2,6-naphthalate by superposing their molecular structures. Comonomer **1** could thus potentially be accommodated in the crystal lattice of PBN if **1** adopted a coplanar geometry, resulting in minimal disruption to the α-PBN crystal. This coplanarity of the biphenyl unit ensures that the required symmetry operation for space group $P\bar{1}$ (an inversion centre) is maintained, as has often been observed in the crystal structures of biphenyl-containing small molecules [18,19].

The novel, rigid, diimide comonomer **1** was obtained in 89% yield from 3,4,3′,4′-biphenyltetracarboxylic dianhydride and 4-aminobutanol. Copoly(ester-imide)s **2**, containing both PBN and comonomer **1**, were synthesised by melt-copolycondensation of **1** with bis(4-hydroxybutyl)-2,6-naphthalate (Scheme 1). Successful copolymerisation was confirmed by ^{1}H and ^{13}C NMR spectroscopy with the actual comonomer ratios of **1** in **2** in the polymers closely matching the feed ratios. The degree of polymerisation was analysed by inherent viscosity and GPC, giving η_{inh} = 0.54–0.69 dL g^{-1} and molecular weights (M_w) in the range 13,000–16,000 Da (Supplementary data, Table S2).

Rotational rheology analysis of the 20 and 25 mol% copolymers of **2** revealed similar viscoelastic properties to those of PBN (Supplementary data, Fig. S5). Upon heating (4 °C min^{-1}, constant frequency of 10 rad s^{-1} and amplitude of 5%) past the T_m, all synthesised materials possess complex viscosities, η*, of <40 Pa s at the extrusion temperature of 290 °C. This suggests facile melt extrusion (which was observed following polycondensation), in accordance with G″ > G′ signifying liquid viscoelastic behaviour. At a constant temperature of 300 °C, shear-thinning is observed with respect to increasing frequency. This may be attributed to increased molecular alignment and the disentanglement of polymer chains. The η* of PBN is also noted to rise proportionally in both temperature and frequency sweep modes, following inclusion of **1**. Although this has no significant consequence on the melt processability of the copolymers **2**, the incorporation of a rigid diimide comonomer has clearly increased the melt viscosity in comparison to PBN, as expected.

DSC cooling scans from the melt were recorded at 20 °C min^{-1} for the PBN homopolymer and for the 20 and 25 mol% copolymers,

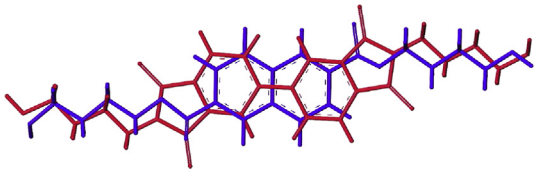

Fig. 1. Superposed molecular structures of bis(4-hydroxybutyl)-2,6-naphthalate (blue) and **1** (red). (For interpretation of the references to colour in this figure legend, the reader is referred to the web version of this article.)

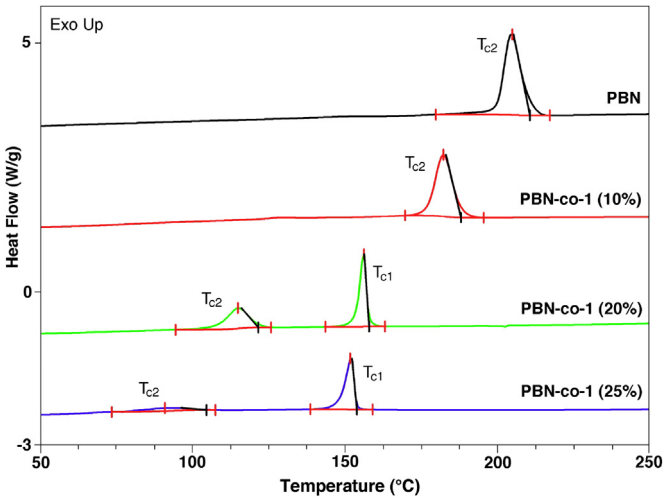

Fig. 2. DSC 1st cooling scans (20 °C min^{-1}) of PBN and of copolymer **2** with 10, 20 and 25 mol% of **1**.

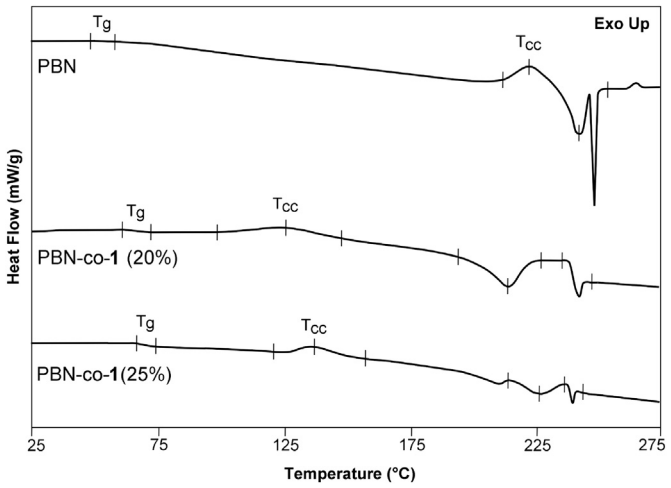

Fig. 4. HyperDSC 2nd heating scans (20 °C min^{-1}) of PBN and **2** containing 20 and 25 mol% of **1** after ballistic cooling.

2, as illustrated in Fig. 1. At this cooling rate it is observed that PBN itself has a single, well-defined crystallisation temperature, T_c, at 209 °C (36.7 J g^{-1}). However, on incorporation of **1** into PBN at levels of 20 and 25 mol%, two major exothermic transitions (the first sharp and the second rather broader) are now seen on cooling at 20 °C min^{-1}. It should also be noted that these two transitions are observed for both copolymers at all cooling rates between 5 and 50 °C min^{-1}.

The higher temperature exotherm, T_{c1}, may be attributed to a transition from the isotropic melt to a mesophase (presumably smectic A) [16], occurring at 156 °C (14.4 J g^{-1}) and 152 °C (12.5 J g^{-1}) for the 20 and 25 mol% copolymers of **2** respectively. The lower temperature exotherm, T_{c2}, is then assigned as a mesophase to crystalline transition, which is progressively depressed upon addition of 20 mol% (115 °C, 11.8 J g^{-1}) and 25 mol% (91 °C, 3.1 J g^{-1}) of comonomer **1** to PBN. For copolymers of **2** containing <20 mol% of **1**, T_{c1} is < T_{c2} resulting in no mesophase formation as the copolymer preferentially undergoes melt-crystallisation. This is illustrated by the cooling scan of the 10 mol% copolymer of **2** (Fig. 2) which shows a melt crystallisation peak (T_{c2}, 182 °C, 28.2 J g^{-1}) that is higher than any possible melt-to-mesophase transition (T_{c1}). The 1st DSC cooling scans are consistent with copolymer **2** being a monotropic liquid crystalline system, in which the metastable mesophase is only observed when direct melt-crystallisation is bypassed by choice of a sufficiently fast cooling rate [16,20].

For the 20 mol% copolymer **2**, a cooling rate from the melt of 250 °C min^{-1} depresses T_{c1} to 141 °C (13.2 J g^{-1}) and T_{c2} is no longer observed (Fig. 3). Thus, the higher cooling rate freezes the copolymer in the mesophase (as a smectic glass) because there is insufficient time for crystallisation to occur below the melt-to-mesophase transition. It should be noted that the copolymer mesophase is isolated at very much lower rates of cooling than the mesophase of PBN itself (which typically requires cooling rates of >20,000 °C min^{-1}) [21], indicating that the copolymer mesophase is significantly slower to crystallise. Isolation of the mesophase is also promoted by the depressed crystallisation temperature of the copolymer containing 20 mol% of **1** (T_{c2} = 115 °C at a cooling rate of 20 °C min^{-1}) which allows the transition from the melt to the mesophase to occur in preference to melt-crystallisation.

Subjecting copolymers **2** to ballistic cooling (approximate rate of 900 °C min^{-1}) from the melt at 300 °C to 0 °C allowed T_gs to be calculated from subsequent heating scans at a reheating rate of 20 °C min^{-1} (Fig. 4 and Table 1). Onset temperatures for T_g were 66 and 74 °C at 20 and 25 mol% incorporation of **1**, the latter affording a 23 °C increase in T_g when compared to PBN itself (51 °C). In addition, the cold crystallisation temperatures, T_{cc}s, for both copolymers of **2** are much lower than that of PBN, indicating a more facile crystallisation upon heating, perhaps templated by the mesophase [22]. This assumes that at least some mesophase is present at the start of the 2nd heating scan, which appears valid when considering that any mesophase-to-crystalline transition (T_{c2}) would be suppressed by the high ballistic cooling rate, as suggested in Fig. 3.

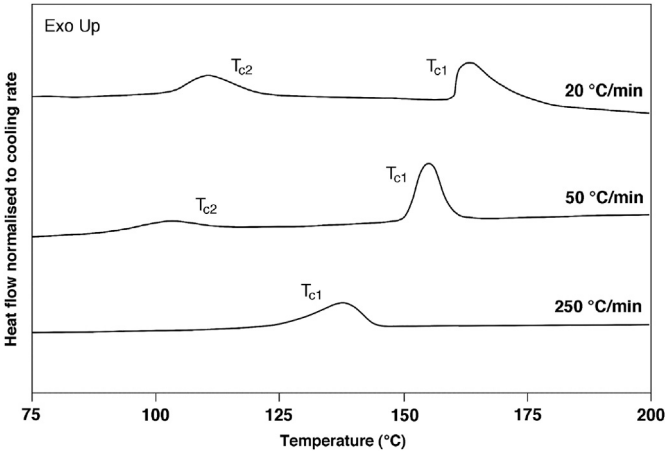

Fig. 3. HyperDSC 1st cooling scans (20, 50, 250 °C min^{-1}) for copolymer **2** containing 20 mol% of **1**. Heatflows have been normalised by dividing by the cooling rate.

Table 1
Thermomechanical properties of PBN and copolymers **2** containing 20 or 25 mol% of comonomer **1**.

Polymer	T_g[a] °C	T_{cc}[a] °C	ΔH_{cc}[a] J g^{-1}	T_{endo}[a] °C	ΔH_{endo}[a] J g^{-1}	G′[b] MPa	G″[c] MPa	E[d] MPa
PBN	51	222	−16.09	242, 247	27.61	735	105	919
PBN-*co*(1)-20	68	126	−12.01	214, 242	23.92	1880	225	988
PBN-*co*(1)-25	74	138	−12.22	226, 240	12.85	2272	240	1221

[a] HyperDSC 2nd heating scan (20 °C min^{-1}).
[b] At 298 K, from DMA temperature sweep (4 °C min^{-1}).
[c] DMA, G″ peak value - see Supplementary data, Fig. S4.
[d] Tensile test at 298 K.

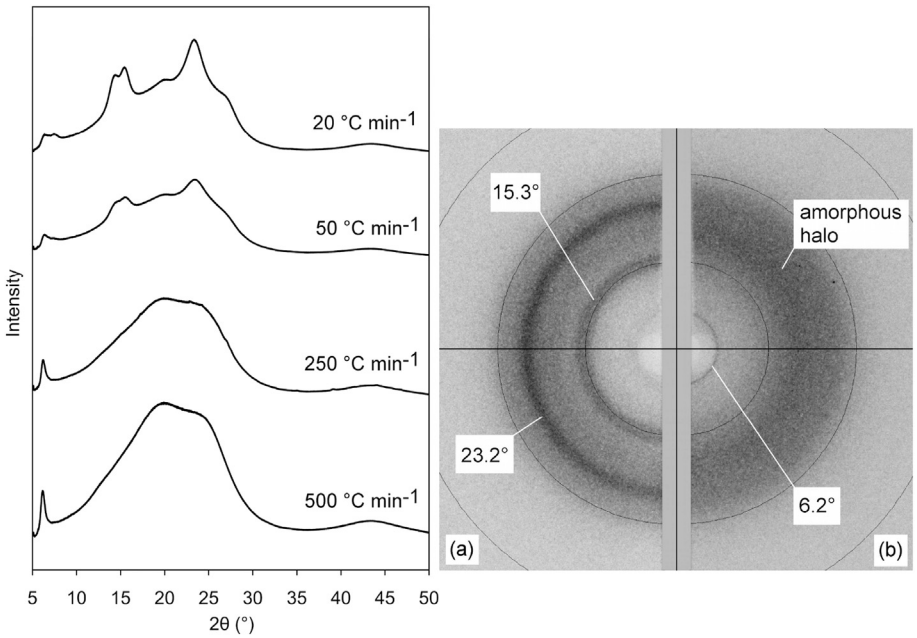

Fig. 5. Comparative X-ray powder diffraction patterns from copolymer **2** containing 20 mol% of **1** after cooling at 20–500 °C min^{-1} (at left), together with comparative X-ray powder diffraction images (at right) from copolymer **2** containing 20 mol% of **1** after cooling at (a) 20 °C min^{-1} and (b) 500 °C min^{-1}. Diffraction angles (2θ) are shown for the main observed rings, and the two inner calibration circles represent *d*-spacings of 6.10 and 3.25 Å.

The measured T_g of PBN itself is 10 °C higher than the literature value of 41 °C quoted for amorphous PBN [23]. It is probable that the higher value seen in the present work is due to incomplete quenching to the amorphous phase of molten PBN, since ΔH_{endo} (the sum of both endotherms observed) is greater than ΔH_{cc}, indicating the presence of some initial crystallinity in PBN at the start of the 2nd heating scan. For the copolymers, the exothermic transition labelled T_{cc} in Fig. 4 is assigned (as noted above) to "cold" crystallisation of the frozen mesophase on heating above the T_g. Multiple melting endotherms are observed both for PBN and for the 20 and 25 mol% copolymers of **2**, but at very much higher temperatures (210–250 °C) than the melt-to-mesophase transition observed at around 150 °C during the copolymer cooling scans. It therefore seems unlikely that any of the melting endotherms seen

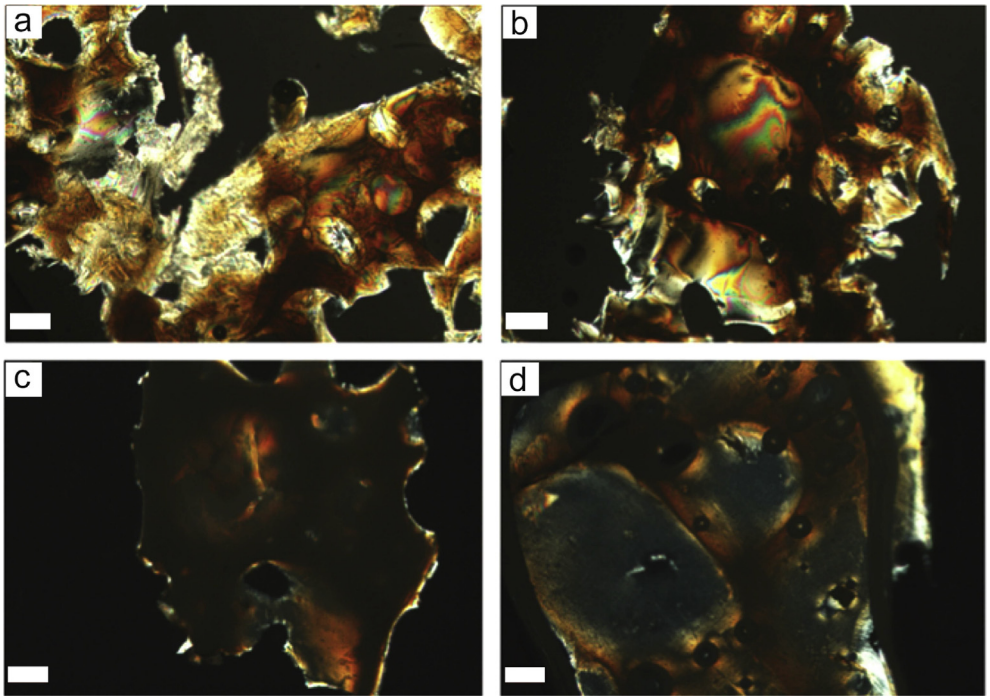

Fig. 6. Polarised optical microscopy images of **2** containing 20 mol% of **1** following cooling rates of: a) 500 °C min^{-1}; b) 250 °C min^{-1}; c) 50 °C min^{-1}; and of PBN: d) 500 °C min^{-1}. Scale bar is 25 μm.

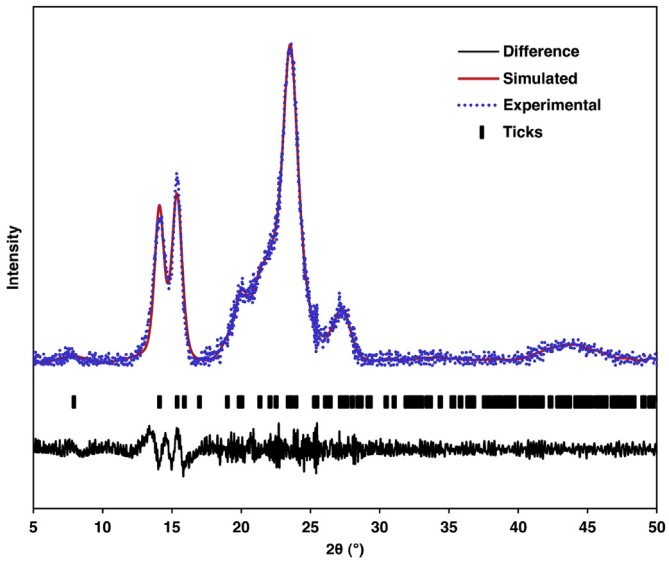

Fig. 7. Rietveld refinement plot of the simulated X-ray powder diffraction pattern for copolymer **2** against the experimental powder diffraction pattern for copolymer **2** containing 20 mol% of **1**. Tick marks indicate reflections predicted by the model.

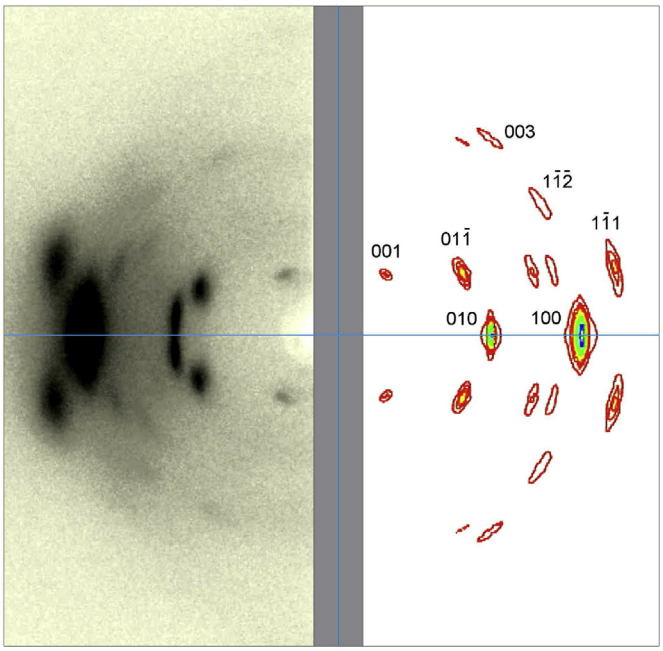

Fig. 8. Simulated X-ray fibre pattern from the optimised model (coloured contour lines, right, with assignments for the major reflections) juxtaposed with the experimental fibre pattern (grayscale, left) for a drawn fibre of copolymer **2** containing 20 mol% of **1**.

in Fig. 4 involves the mesophase. Instead, we suggest that the lower-temperature endotherm corresponds to the melting of thin, lamellar crystallites formed during cold crystallisation, with the final, high-temperature endotherm being associated with thicker lamellae produced either on cooling from the melt or by recrystallisation of the thinner lamellae on heating [24].

Incorporation of the rigid, diimide comonomer **1** also increases the mechanical stiffness of the copolymer relative to PBN, with both the 20 and 25 mol% copolymers of **2** exhibiting increased storage, loss and elastic moduli (Table 1). It is probable that the enhanced moduli primarily originate from the inclusion of a more rigid co-unit, while retaining efficient chain orientation as in PBN.

Confirmation of a frozen mesophase in copolymer **2** was achieved by X-ray powder diffraction analysis of samples containing 20 mol% of comonomer **1** after cooling at rates between 20 °C and 500 °C min^{-1}. The change from a semi-crystalline copolymer to a liquid crystalline material as the cooling rate increases is very evident in Fig. 5. The clear diffraction peaks at $2\theta = 15.3$ and 23.2°, seen on cooling at 20 °C min^{-1}, merge into an amorphous halo on cooling at 250 °C min^{-1}, in agreement with the HyperDSC traces shown in Fig. 3 where the copolymer mesophase is quenched at cooling rates >50 °C min^{-1}. Conversely, a very sharp diffraction peak at low angle ($2\theta = 6.2°$) begins to emerge at a cooling rate of 50 °C min^{-1}, and becomes more prominent at faster cooling rates. This peak may be attributed to the smectic layers of the copolymer mesophase, corresponding to a layer spacing of ca. 14.1 Å.

Polarised optical microscopy on ballistic-cooled samples of **2** containing 20 mol% of **1** gave additional evidence for a copolymer mesophase [25]. Birefringence, together with some indication of a Schlieren texture, is evident for the 20 mol% copolymer of **2** cooled at 500 °C min^{-1} and at 250 °C min^{-1} (Fig. 6a and b). In contrast, when the same copolymer is cooled at 50 °C min^{-1} and therefore allowed to melt-crystallise after mesophase formation (Fig. 3), the sample is largely opaque (Fig. 6c), denoting a semi-crystalline material. For comparison, PBN itself is crystalline and opaque when cooled at 500 °C min^{-1} (Fig. 6d), because the PBN mesophase is inaccessible even at this cooling rate. Thus, PBN itself does not show birefringence associated with a mesophase, in contrast to samples of the 20 mol% copolymer of **2** cooled at the same rate.

The X-ray powder diffraction pattern for the 20 mol% copolymer of **2** after melt-crystallisation (Fig. 5) differs in detail from those reported for α- and β-PBN (see Supplementary data, Fig. S2), although the copolymer pattern has broadly similar features to that of the α-phase. The retention of thermal crystallisability, even at 20 and 25 mol% of **1** suggests that cocrystallisation is indeed occurring in the copolymers. However, in contrast to the analogous *PEN*-based copoly(ester-imide) [17], it seems that no radical change in structure occurs – the copolymer crystal structure is provisionally identified as a variant of the α-phase (with small changes to the unit cell parameters but no change in space group) by X-ray powder and fibre diffraction, interfaced to computational modelling and diffraction simulation.

The crystal structure of **2** was initially modelled as a polymorph of α-PBN, assuming that the diffraction pattern of the model would not be drastically affected by the absence of comonomer units. As a control, the powder diffraction pattern for α-PBN was simulated using literature unit cell dimensions and atomic coordinates [26], and was found to be in very good agreement with an experimental powder pattern obtained from PBN synthesised in the present work. Adjustment of the α-PBN unit cell within boundary limits defined by both α- and β-PBN crystal structures lead to an extremely promising initial match between the simulated diffraction pattern and an experimental pattern for copolymer **2** containing 20 mol% of **1**. On this basis, the unit cell dimensions of **2** were provisionally set at $a = 4.74$, $b = 6.37$, $c = 14.47$ Å, $\alpha = 105.8$, $\beta = 122.3$, $\gamma = 98.5°$.

Pawley and Rietveld refinement ($R_{wp} = 9\%$ and 12% respectively) of the preliminary crystal structure of **2** with respect to the experimental powder diffraction pattern of copolymer **2** containing 20 mol% of **1** (Fig. 7) gave a final model in space group $P-1$, $a = 4.74$, $b = 6.38$, $c = 14.45$ Å, $\alpha = 106.1$, $\beta = 122.1$, $\gamma = 97.3°$, $\rho = 1.37$ g cm^{-3}. A fibre pattern simulated from this proposed copolymer crystal structure is in very good agreement with the experimental fibre pattern (Fig. 8), thus further demonstrating the

validity of the computational model. As also seen in the fibre diffraction pattern of the analogous PEN-based copolymer [15], experimental reflections for **2** (specifically 001, 01-1 and 1-11) are displaced above and below the layer lines, a characteristic feature of diffraction from copolymer crystallites containing random-sequence chains. [27], [28].

4. Conclusions

We report the synthesis of a novel biphenyldiimide comonomer **1** in excellent yield from commercially available starting reagents, and the subsequent production of copoly(ester-imide)s **2** with PBN. Incorporation of 20 and 25 mol% of **1** results in increased glass transition temperatures, unusually high retention of semi-crystalline character, and facile access to a liquid crystalline phase, depending on processing conditions. Structural analysis by X-ray powder diffraction interfaced to computational modelling has enabled a provisional crystal structure for copolymer **2** to be identified and rationalised in terms of isomorphism between the naphthalate-diester and biphenyldiimide comonomers.

Acknowledgements

We thank Dr Kenneth Shankland for help with processing X-ray powder diffraction data, and Mr Nick Spencer and Ms Jessica Chappell for technical assistance. The research was funded by DuPont Teijin Films UK (studentship awards to SMJ and SJM), the Royal Society of London (a Brian Mercer feasibility award to HMC, grant MF130002) and the Engineering and Physical Sciences Research Council of the United Kingdom (a Doctoral Training Grant to SJM).

Appendix A. Supplementary data

Supplementary data related to this article can be found at http://dx.doi.org/10.1016/j.polymer.2015.05.025.

References

[1] W. MacDonald, Polym Int 51 (2002) 923–930.
[2] Soichiro H. Japanese Pat. Appln. 2010; JP2010013599 (A), to Teijin Fibres Ltd.
[3] C.L. Mares, J De Abajo, Angew Makromol Chem 55 (1975) 73–83.
[4] J.U.N. Xiao, X. Wan, D. Zhang, Q. Zhou, S.R. Turner, J Polym Sci Chem 39 (2001) 408–415.
[5] S. Maiti, S.J. Das, Appl Sci 26 (1981) 957–978.
[6] H. Ma, M. Hibbs, D.M. Collard, D.A. Schiraldi, Macromolecules 35 (2002) 5123–5130.
[7] Y.S. Hu, R.Y.F. Liu, M. Rogunova, D.A. Schiraldi, S. Nazarenko, A. Hiltner, et al., J Polym Sci B Polym Phys 40 (2002) 2489–2503.
[8] L.E.E.S. Park, D.C. Lee, Polym Eng Sci 35 (1995) 1629–1635.
[9] L.J.F. Mary, P. Kannan, Polym Int 47 (1998) 317–323.
[10] G.Z. Papageorgiou, G.P. Karayannidis, Polymer 42 (2001) 8197–8205.
[11] Y.G. Jeong, W.H. Jo, S.G. Lee, Macromolecules 33 (2000) 9705–9711.
[12] D.A. Schiraldi, in: J. Scheirs, T.E. Long (Eds.), Modern polyesters: chemistry and technology of polyesters and copolyesters, John Wiley, Chichester, 2003, pp. 245–266.
[13] R.R. Gallucci, B.R. Patel, in: J. Scheirs, T.E. Long (Eds.), Modern polyesters: chemistry and technology of polyesters and copolyesters, John Wiley, Chichester, 2003, pp. 293–332.
[14] D.D. Callander, in: J. Scheirs, T.E. Long (Eds.), Modern polyesters: chemistry and technology of polyesters and copolyesters, John Wiley, Chichester, 2003, pp. 323–333.
[15] M. Ju, J. Huang, F. Chang, Polymer 43 (2002) 2065–2074.
[16] T. Konishi, K. Nishida, G. Matsuba, T. Kanaya, Macromolecules 41 (2008) 3157–3161.
[17] S.J. Meehan, S.W. Sankey, S.M. Jones, W.A. MacDonald, H.M. Colquhoun, ACS Macro Lett 3 (2014) 968–971.
[18] H.M. Colquhoun, C.A. O'Mahoney, D.J. Williams, Polymer 34 (1993) 218–221.
[19] C.P. Brock, R.P. Minton, J Am Chem Soc 111 (1989) 4586–4593.
[20] S.O. Kim, C.M. Koo, I.J. Chung, H. Jung, Macromolecules 34 (2001) 8961–8967.
[21] D. Cavallo, D. Mileva, G. Portale, L. Zhang, L. Balzano, G.C. Alfonso, et al., ACS Macro Lett 1 (2012) 1051–1055.
[22] A.J. Jing, O. Taikum, C.Y. Li, F.W. Harris, Z.D. Cheng, Polymer 43 (2002) 3431–3440.
[23] T. Yamanobe, H. Matsuda, K. Imai, A. Hirata, S. Mori, T. Komoto, Polymer 28 (1996) 177–181.
[24] Y. Shi, A. Saleh, A.J. Jabarin, Appl Polym Sci 81 (2001) 11–22.
[25] S.T. Wu, Phys Rev A 33 (1986) 1270–1274.
[26] H. Koyano, Y. Yamamoto, Y. Saito, T. Yamanobe, T. Komoto, Polymer 39 (1998) 4385–4391.
[27] G.A. Gutierrez, J. Blackwell, R.A. Chivers, Polymer 26 (1986) 348–354.
[28] Z. Sun, H.M. Cheng, J. Blackwell, Macromolecules 24 (1991) 4162–4167.